

Magnetopolaron effect on shallow donors in GaAs

J.-P. Cheng* and B. D. McCombe†

Department of Physics and Astronomy, State University of New York at Buffalo, Buffalo, New York 14260

J. M. Shi, F. M. Peeters, and J. T. Devreese

Department of Physics, University of Antwerp (UIA), Universiteitsplein 1, B-2610 Antwerpen, Belgium

(Received 26 April 1993)

Low-temperature experimental measurements and variational calculations of the transition energies of shallow donor (Si) impurities in bulk GaAs as a function of magnetic field throughout the resonant polaron region are reported. Far-infrared photoconductivity spectra in magnetic fields up to 23.5 T show several anti-level-crossing processes at energies above the LO-phonon energy, clearly demonstrating the resonant interactions between GaAs LO phonons and impurity-bound electrons involving several excited impurity states. Very good agreement is obtained between experiment and calculated transition energies throughout the resonant region with the accepted value of the Fröhlich coupling constant ($\alpha=0.068$). The effects of uncertainties in the measured values of the dielectric constants (thus the value of α) are studied in the calculation, and the implication of these results for similar studies in GaAs/Al_xGa_{1-x}As quantum wells is discussed.

INTRODUCTION

Much work, both experimental and theoretical, has been devoted recently to the investigation of the electron-phonon interaction in reduced-dimensional systems, such as semiconductor heterostructures, quantum wells, and superlattices.¹⁻⁷ Some of these investigations have been on quasi-two-dimensional (2D) systems with a large density of free electrons,¹ which complicates the interpretation due to possible screening and Pauli principle effects.⁵ An inherent single-particle system, which is free of such complications, involves shallow hydrogenic donors, and recent investigations of such systems in GaAs/Al_xGa_{1-x}As multiple-quantum-well (MQW) structures² have been interpreted in terms of both Fröhlich interaction with bulk (3D) longitudinal-optical (LO) phonons,⁶ as well as with confined and interface optical modes.⁷ A crucial feature in these interpretations is the magnitude of the resonant interaction which takes place when the electronic transition is tuned into resonance (by an applied magnetic field) with the optical modes. In the structures investigated these questions are basically quantitative ones, which depend both on the magnitude of the Fröhlich coupling constant α and the choice of variational trial functions for the calculations. The latter point is particularly important for variational calculations since the splittings at the various resonances involve matrix elements of the interaction Hamiltonian between excited-state wave functions, which are likely to be less accurate than the expectation values in, e.g., the ground state. Thus it is important to obtain some indication of the accuracy of the trial functions and the dependence of the results upon the value of the coupling constant (which has some range of uncertainty as discussed below) and upon the trial wave functions for a system in which the phonon modes and the form of the interaction is well known. The ideal system for this is shallow

donors in bulk GaAs. To our knowledge, the present work is the first experimental work on the resonant interaction of donors with optical phonons in bulk GaAs. In the following sections we present a detailed experimental study of the resonant interaction of shallow Si donors in a "thick" epitaxial GaAs layer in magnetic fields up to 23.5 T; these results are compared with variational calculations involving two different sets of trial wave functions, and the dependence of the results in the resonant region on the value of α is examined. These dependences are discussed, and the general validity of various interpretations of such experiments on MQW structures is examined.

EXPERIMENT

The sample used in this work is a 10- μ m-thick epitaxial layer grown by molecular-beam epitaxy on a semi-insulating GaAs buffer layer and doped with silicon donors at a nominal concentration of $2 \times 10^{14}/\text{cm}^3$. Ohmic contacts were made by indium diffusion, and the photoconductive ac voltage signal was obtained by passing a constant current through the sample and chopping the incident far-infrared (FIR) light. Magneto-optical spectra were obtained with Fourier-transform spectrometers in conjunction with a 9-T superconducting magnet (at Buffalo) or a 23-T Bitter magnet (at the Francis Bitter National Magnet Laboratory). FIR light was guided from the spectrometer to the sample by light-pipes, reflecting mirrors, and condensing light-cone optics. All data were taken at liquid-He temperatures in the Faraday geometry, in which the FIR light was intentionally guided with its propagation direction parallel to the magnetic field. However, a small fraction of the light incident on the sample propagates at a small angle to the magnetic field due to the nature of the condensing light cone that is placed immediately before the sample.

THEORETICAL

Our theoretical analysis is based on the standard effective-mass approximation, and in the absence of electron-LO-phonon interaction it is described by the Hamiltonian

$$H_e = \frac{1}{2m^*} \left[\mathbf{p} + \frac{e\mathbf{A}}{c} \right]^2 - \frac{e^2}{\epsilon_0 r}, \quad (1)$$

where $\mathbf{A} = (-By/2, Bx/2, 0)$ is the vector potential, which we have expressed in the symmetric gauge. In the following we use the effective Rydberg $R^* = e^2/2\epsilon_0 a^*$ as the unit of energy, $a^* = \epsilon_0 \hbar^2/m^* e^2$ as the unit of length, and $\gamma = \hbar e B/2m^* c R^*$ as the dimensionless unit of magnetic field. The Schrödinger equation corresponding to the Hamiltonian of Eq. (1) cannot be solved exactly; therefore we relied on a variational calculation for the donor states. We used the trial wave functions

$$\psi_{nmp}(\rho, \varphi, z) = \rho^{|m|} |z\rangle^p e^{im\varphi} e^{-\xi\rho^2 - \zeta\sqrt{\rho^2+z^2}}, \quad (2)$$

where ξ and ζ are two variational parameters which minimize the unperturbed energy of the donor state Ψ_{nmp} ,

$$E_{nmp}^0 = \frac{\langle \psi_{nmp} | H_e | \psi_{nmp} \rangle}{\langle \psi_{nmp} | \psi_{nmp} \rangle}. \quad (3)$$

We have compared the resulting binding energies and have found them to be within 1.6% of an exact numerical solution^{8,17} of Eq. (1). The $1s \rightarrow 2p_{+1}$ transition energies are within 0.2% of this exact numerical calculation. We also tried a wave function with three variational parameters where we replaced $\exp\{-\zeta[\rho^2+z^2]^{1/2}\}$ by $\exp\{-\xi[\rho^2+\delta^2 z^2]^{1/2}\}$ in Eq. (2). We found that this improves the $1s \rightarrow 2p_{+1}$ transition energy by 0.13% at most in the intermediate magnetic-field region. For small and large magnetic fields the improvement is negligible. For the considered experimental situation it is sufficient to include the following states in the calculation: $1s = |1, 0, 0\rangle$, $2p_{\pm 1} = |2, \pm 1, 0\rangle$, $2p_0 = |2, 0, 1\rangle$, $3d_{-2} = |3, -2, 0\rangle$, and $4f_{-3} = |4, -3, 0\rangle$.

In order to incorporate the polaron correction we use second-order perturbation theory which gives

$$\Delta E_{nmp} = - \sum_{ijk} \sum_{\mathbf{q}} \frac{|\langle ijk; \mathbf{q} | H_I | nmp; 0 \rangle|^2}{\hbar\omega_{\mathbf{q}} + E_{ijk}^0 + E_{nmp}^0 + \Delta E_{nmp}}. \quad (4)$$

H_I is the electron-phonon interaction Hamiltonian given by

$$H_I = \sum_{\mathbf{q}} (V_{\mathbf{q}} a_{\mathbf{q}} e^{i\mathbf{q}\cdot\mathbf{r}} + V_{\mathbf{q}}^* a_{\mathbf{q}}^\dagger e^{-i\mathbf{q}\cdot\mathbf{r}}). \quad (5)$$

Here $a_{\mathbf{q}}^\dagger$ ($a_{\mathbf{q}}$) is the creation (annihilation) operator of a LO phonon with wave vector \mathbf{q} and energy $\hbar\omega_{\mathbf{q}}$,

$$|V_{\mathbf{q}}|^2 = \frac{4\pi\alpha}{V} \left[\frac{\hbar}{2m^* \omega_{\text{LO}}} \right]^{1/2} \left[\frac{\hbar\omega_{\text{LO}}}{q} \right]^2, \quad (6)$$

with V the volume of the system, and

$$\alpha = \frac{e^2}{\hbar} \left[\frac{m^*}{2\hbar\omega_{\text{LO}}} \right]^{1/2} \left[\frac{1}{\epsilon_\infty} - \frac{1}{\epsilon_0} \right] \quad (7)$$

is the dimensionless coupling constant with ϵ_0 and ϵ_∞ the static and high-frequency dielectric constants, respectively. The state $|i, j, k; \mathbf{q}\rangle$ describes an electron with unperturbed energy E_{ijk}^0 and a LO phonon with momentum $\hbar\mathbf{q}$ and energy $\hbar\omega_{\mathbf{q}}$. To describe the resonant magnetopolaron effect it is necessary to rely on improved Wigner-Brillouin perturbation theory,^{4,9} which implies that we have to use

$$\Delta_{nmp} = \Delta E_{nmp} - \Delta E_{1s} \quad (8)$$

in Eq. (4).

We know that in high magnetic fields band nonparabolicity is important for the donor energy levels. We used the standard Kane model¹⁰

$$E_{\text{np}} = \frac{E_g}{2} \left[-1 + \left(1 + 4 \frac{E_p}{E_g} \right)^{1/2} \right] \quad (9)$$

in order to obtain the energies of the nonparabolic conduction band (E_{np}) from the energies in a parabolic conduction band (E_p). For the band gap we took $E_g = 1520$ meV. The Kane model has been proven¹¹ to be successful in describing the band nonparabolicity in GaAs.

RESULTS AND DISCUSSION

Photoconductivity spectra of the impurity transitions at several magnetic fields (low-field region) are shown in Fig. 1. In this field region all features in the spectra can be clearly identified by comparison with previous experimental work¹² and theoretical calculations.¹³ At zero magnetic field the strongest peak at 35.5 cm^{-1} in the spectrum is comprised of $1s \rightarrow 2p_{\pm 1}$ and $1s \rightarrow 2p_0$ transi-

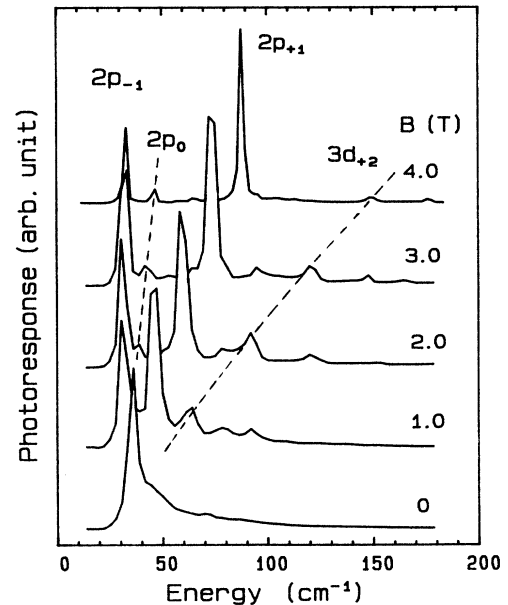


FIG. 1. Photoconductivity spectra at several magnetic fields (low-field region). Major transition peaks are labeled by comparison with previous experimental and theoretical work (Refs. 12 and 13).

tions which are degenerate. As the field is increased, the peak splits into three lines. In the spectrum of 4 T, the strongest line at 88 cm^{-1} is the $1s \rightarrow 2p_{+1}$ transition, the second strongest line at 34 cm^{-1} is the $1s \rightarrow 2p_{-1}$ transition, and the weaker line at an energy $\sim 13 \text{ cm}^{-1}$ higher than the $1s \rightarrow 2p_{-1}$ line is the $1s \rightarrow 2p_0$ transition. The latter is electric dipole allowed for the FIR E field polarized along the magnetic field; it is observed in these experiments only because all of the FIR radiation does not propagate exactly along the direction of the magnetic field due to the condensing-cone optics. Other, even weaker, features are due to transitions from the ground ($1s$) state to other excited states (such as $3d_{+2}$), which we will not discuss in this paper.

The $1s \rightarrow 2p_{+1}$ transition can be tuned by magnetic field through the resonance energy region with GaAs optical phonons. Figure 2 shows the photoconductivity spectra of impurity transitions in the resonant magnetopolaron region. As magnetic field increases, the state $|2p_{+1}, 0\text{-phonon}\rangle$ crosses the state $|1s, 1\text{-phonon}\rangle$. A typical antilevel crossing behavior for the relative intensities of the lower and higher branches can be clearly observed at fields near 18 T due to the resonant electron-LO-phonon interaction. Notice that the 18-T spectrum appears much noisier than other spectra; this is due to the fact that the $1s \rightarrow 2p_{+1}$ transition is very close to the reststrahlen band and the entire spectrum is dominated in this case by the $1s \rightarrow 2p_{-1}$ and $1s \rightarrow 2p_0$ transitions at much lower energies (not shown in the figure); thus the vertical scale is expanded for this spectral region for a clearer comparison. Above 18.5 T the upper branch becomes the strongest line in the spectra, and the lower branch completely disappears. Meanwhile, several weak

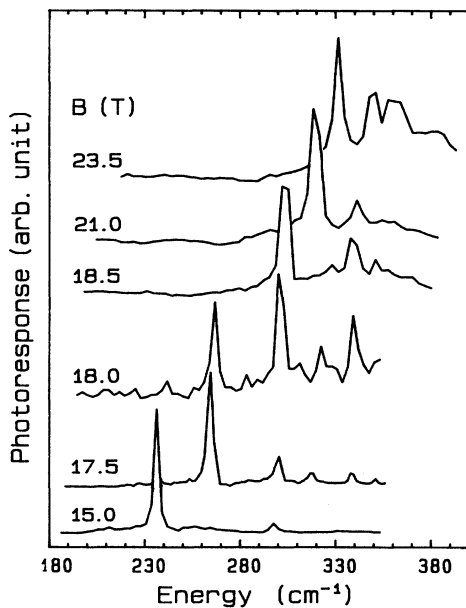


FIG. 2. Photoconductivity spectra for the $1s-2p_{+1}$ transition at several magnetic fields in the resonant magnetopolaron region. The 18-T spectrum has been expanded for clarity of comparison.

features appear in the highest-energy region of the spectra. These transitions have been attributed to resonant coupling of the $|2p_{+1}, 0\text{-phonon}\rangle$ state to other excited states, $|2p_{-1}, 1\text{-phonon}\rangle$, $|3d_{-2}, 1\text{-phonon}\rangle$, $|4f_{-3}, 1\text{-phonon}\rangle$, and $|2p_0, 1\text{-phonon}\rangle$, via the electron-phonon interaction (see discussion below). At the highest magnetic fields, the relative intensities of these features become stronger, since the $|2p_{+1}, 0\text{-phonon}\rangle$ state is crossing those excited states in this field region.

In Fig. 3 we plot experimental transition energies for several impurity transitions as a function of magnetic field (dots). In the resonant polaron region six branches are clearly observed which result from virtual interactions with the LO phonons. Theoretical calculations (solid lines) are also presented in this figure for comparison. In the numerical analysis we use the approach of Ref. 14 (see also Ref. 17) for the nonresonant polaron correction in the low magnetic-field region. In the resonant polaron region (high magnetic fields) the perturbation theory outlined in the preceding section is used. These two methods yield nearly identical results in the intermediate field region. The following parameters were used in the calculation: $m^*/m_0=0.067$, $\epsilon_0=12.75$, $\hbar\omega_{LO}=296 \text{ cm}^{-1}$, $\alpha=0.068$. Notice that the measured low-temperature value of ϵ_0 has an uncertainty region from 12.14 to 12.8;¹⁵ however, our choice of ϵ_0 gives good agreement with observed $1s \rightarrow 2p$ transitions at low magnetic fields when the polaron corrections are considered. For example, at zero magnetic field the measured $1s \rightarrow 2p$ transition energy is 35.5 cm^{-1} , and the calculation gives 33.9 cm^{-1} without polaron correction and 35.4 cm^{-1} with the correction. The value of coupling constant α is

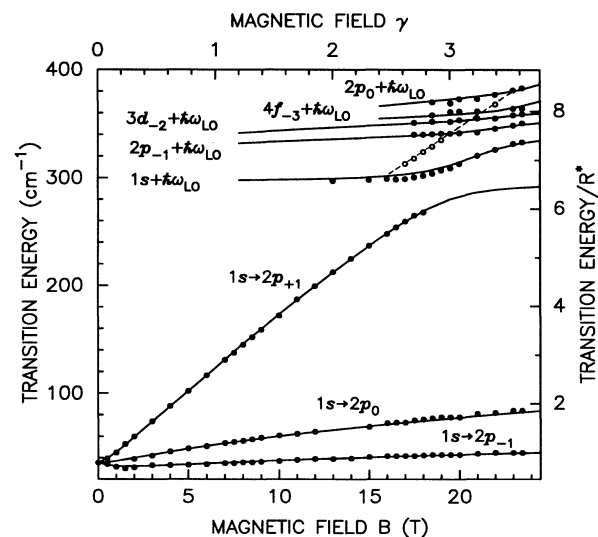


FIG. 3. Transition energy as a function of magnetic field for several major impurity transitions. The solid dots are experimental data; the solid curves are variational calculations of magnetopolaron effects on shallow impurities with $\alpha=0.068$. An unidentified transition is indicated by open circles and a dashed line. Experimental precision in peak position is less than the size of the dots.

determined by Eq. (7), where ϵ_∞ is determined from the Lyddane-Sachs-Teller (LST) relation with $\epsilon_0/\epsilon_\infty = (\omega_{LO}/\omega_{TO})^2 = 1.17$ (corresponding to the TO-phonon energy $\hbar\omega_{TO} = 273.5 \text{ cm}^{-1}$). Hence, there is no adjustable parameter in the calculation. (See below for a discussion of the effects of varying α on the results.) Overall, the calculations are in very good agreement with experimental results for all transitions in the whole magnetic-field region of the experiment. The largest discrepancy occurs for the $1s + \hbar\omega_{LO}$ branch in the region just above the LO-phonon energy; the experimental points are below the theoretical line by a maximum of $4\text{--}5 \text{ cm}^{-1}$ between 16 and 20 T. This systematic deviation may result from dielectric effects in the optical response in this spectral region, which is very close to $\hbar\omega_{LO}$ (the upper edge of the reststrahlen band). The four highest-energy branches have been identified as the resonant branches of $2p_{-1} + \hbar\omega_{LO}$, $3d_{-2} + \hbar\omega_{LO}$, $4f_{-3} + \hbar\omega_{LO}$, and $2p_0 + \hbar\omega_{LO}$, and we believe that this is the first time that the transitions have been observed in bulk GaAs. In addition to these resonant branches, a nonresonant feature is observed at energies above the LO-phonon energy, as indicated by the open circles and the dashed line. This feature increases linearly in energy with increasing magnetic field, and the origin of this transition is not clear at present.

From the definition of α [see Eq. (7)] we notice that α is determined by the values of the dielectric constants, ϵ_0 and ϵ_∞ . Experimental uncertainties in the low-temperature values of ϵ_0 and ϵ_∞ will induce uncertainties in α and consequently in the strength of the polaron effects. From Ref. 15, the LST relation gives values of $\epsilon_0/\epsilon_\infty$ between 1.166 and 1.183 from experimentally measured optical-phonon energies at low temperatures. Thus α has a corresponding uncertainty region between 0.064

and 0.072. To study the effects of this uncertainty in α on the resonant polaron corrections, the resonant interaction region in Fig. 3 has been enlarged in Fig. 4, and three calculated curves with different values of the Fröhlich coupling constant are shown in the figure; the dotted curves are for $\alpha=0.064$, the solid curves for $\alpha=0.068$, and the dashed curves for $\alpha=0.072$. There is *no significant difference* between these three curves in this energy region, although the reduced coupling-constant value (dotted curves) slightly improves the agreement between the theory and experiment for the $1s + \hbar\omega_{LO}$ branch. This result might be understood by considering the case of resonant polaron effects for free-electron Landau levels, where the energy splitting at resonance ($N=1$ Landau level crossing the energy of $N=0$ level plus one phonon) is proportional to $\alpha^{2/3}$. For about 12% change in α , the relative change in the resonant splitting is about 8%, which is only $2\text{--}3 \text{ cm}^{-1}$ for a roughly 30-cm^{-1} total-energy splitting. As a consequence an accurate determination of the coupling constant from the polaron resonance splitting is quite difficult.

CONCLUSION

Resonant electron-LO-phonon interaction has been clearly observed for shallow donors in GaAs polar semiconductor with no complications of screening and occupation effects which are encountered in the free-electron cyclotron resonance experiments in quasi-2D systems. The complex resonant branches above the GaAs LO-phonon energy result from interactions involving several excited impurity states, and they provide more reliable data for the resonant polaron effects since they are free from possible dielectric artifacts due to the reststrahlen band. The energy splittings at and above the LO-phonon energy are a measure of the electron-LO-phonon coupling strength and are well described by our variational calculations with the accepted value of coupling constant ($\alpha=0.068$) in the Fröhlich interaction Hamiltonian. When the coupling constant is changed within the allowed range as given by the uncertainties of the dielectric-constant measurements at low temperatures, our calculation shows no significant change in the transition energies in the resonant polaron region.

These *same* selected parameters (dielectric constants and Fröhlich coupling constant) that result in a best fit to the resonant polaron data in bulk GaAs should be used in the calculation for the quasi-2D systems when the model of a 2D electron interacting with bulk (3D) LO phonons is used in order to clarify the different interpretations of the observed enhancement in the polaron effects in the confined structures.¹⁶ At present, it is clear that the electronic wave-function confinement is the major contribution to the enhanced polaron effects since the energy splitting at resonance is not very sensitive to the value of coupling constant in the Fröhlich Hamiltonian. However, the subtle differences between the calculated results of different interaction mechanisms, namely the electron-interface (confined)-phonon interactions versus the electron-bulk-LO-phonon interactions, are still not resolved with the existing experimental results.

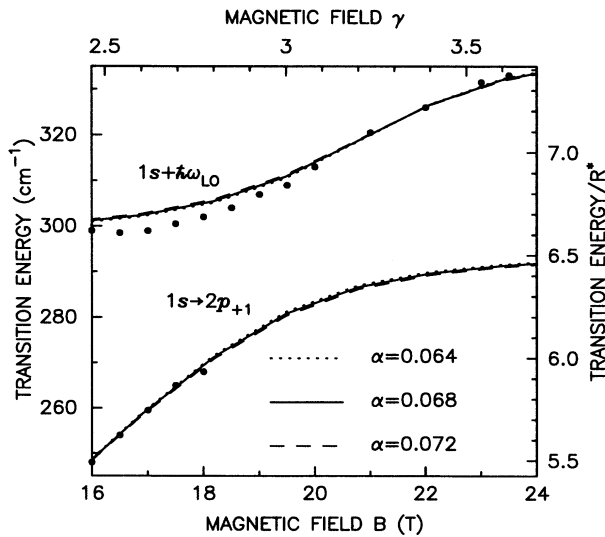


FIG. 4. Expansion of the resonant polaron region of Fig. 3. The dotted curves are calculations with $\alpha=0.064$, the solid curves are for $\alpha=0.068$, and the dashed curves are for $\alpha=0.072$.

ACKNOWLEDGMENTS

We are very grateful to S. Holmes for providing the sample. The high magnetic-field measurements were carried out at the Francis Bitter National Magnet Laboratory; we thank all of the staff, especially B. Brandt and L. Rubin, for assistance. J.P.C. and B.D.M. thank the

Office of Naval Research for support under Grant No. N00014-89-J-1673. The theoretical work was sponsored by "Diensten voor de Programmatie van het Wetenschapsbeleid" under Contract No. IT/SC/24. One of us (F.M.P.) was supported by the Belgian National Science Foundation.

*Present address: Francis Bitter National Magnet Laboratory, Massachusetts Institute of Technology, Cambridge, MA 02139.

†Visiting scientist of Francis Bitter National Magnet Laboratory.

¹M. Horst, U. Merkt, and J. P. Kotthaus, *Phys. Rev. Lett.* **50**, 754 (1983); W. Seidenbusch, G. Lindemann, R. Lassnig, J. Edlinger, and E. Gornik, *Surf. Sci.* **142**, 375 (1984); C. J. G. M. Langerak, J. Singleton, P. J. van der Wel, J. A. A. J. Perenboom, D. J. Barnes, R. J. Nicholas, M. A. Hopkins, and C. T. P. Foxon, *Phys. Rev. B* **38**, 13 133 (1988).

²Y. H. Chang, B. D. McCombe, J.-M. Mercy, A. A. Reeder, J. Ralston, and G. A. Wicks, *Phys. Rev. Lett.* **61**, 1408 (1988); S. Huant, W. Knap, G. Martinez, and B. Etienne, *Europhys. Lett.* **7**, 159 (1988); J.-P. Cheng, B. D. McCombe, and G. Brozak, *Phys. Rev. B* **43**, 9324 (1991).

³S. Das Sarma, *Phys. Rev. Lett.* **52**, 859 (1984).

⁴F. M. Peeters and J. T. Devreese, *Phys. Rev. B* **31**, 3689 (1985).

⁵D. M. Larsen, *Phys. Rev. B* **30**, 4595 (1984); S. Das Sarma and B. A. Mason, *ibid.* **31**, 5536 (1985); X. Wu, F. M. Peeters, and J. T. Devreese, *ibid.* **34**, 2621 (1986).

⁶J. M. Shi, F. M. Peeters, G. Q. Hai, and J. T. Devreese, *Phys.*

Rev. B **44**, 5692 (1991).

⁷D. L. Lin, R. Chen, and T. F. George, *Phys. Rev. B* **43**, 9328 (1991).

⁸H. C. Praddaude, *Phys. Rev. A* **6**, 1321 (1972).

⁹G. Lindemann, R. Lassnig, W. Seidenbusch, and E. Gornik, *Phys. Rev. B* **28**, 4693 (1983).

¹⁰G. Ambrzevicins and M. Cardona, *Phys. Rev. Lett.* **63**, 2288 (1989).

¹¹F. M. Peeters, X. G. Wu, J. T. Devreese, C. J. G. M. Langerak, J. Singleton, D. J. Barnes, and R. J. Nicholas, *Phys. Rev. B* **45**, 4296 (1992).

¹²See, e.g., C. J. Armistead, R. A. Stradling, and Z. Wasilewski, *Semicond. Sci. Technol.* **4**, 557 (1989).

¹³P. C. Makado and N. C. McGill, *J. Phys. C* **19**, 873 (1986).

¹⁴D. M. Larsen, *J. Phys. Chem. Solids* **29**, 271 (1968).

¹⁵See, e.g., *Key Papers in Physics: Gallium Arsenide*, edited by J. S. Blackmore (AIP, New York, 1987), and references therein.

¹⁶J.-P. Cheng, B. D. McCombe, and G. Brozak, *Surf. Sci.* **267**, 488 (1992); J.-P. Cheng, B. D. McCombe, G. Brozak, and W. Schaff (unpublished).

¹⁷J. M. Shi, F. M. Peeters, and J. T. Devreese, *Phys. Rev. B* (to be published).